doi:10.6041/j.issn.1000-1298.2016.02.038

Factors Affecting Dynamic Laser Speckle Activity of Beef

Dong Qingli Jin Man Hu Menghan Liu Baolin
(*School of Medical Instrument and Food Engineering*, *University of Shanghai for Science and Technology*, *Shanghai* 200093, *China*)

Abstract: Dynamic laser speckle technique, also termed as dynamic biospeckle, is a portable and non-invasive as well as low-cost screening tool for online or point-of-sale applications in agricultural products. A custom made dynamic laser speckle system mainly consisted of a He-Ne laser generator operating at four wavelengths of 405 nm, 520 nm, 635 nm and 780 nm, respectively, an industrial CMOS camera for the sequential images acquisition, a computer and a height adjustable sample stage. The lighting and imaging units were placed into an illumination chamber to avoid the interference of natural light. In order to optimize the measurement conditions of dynamic laser speckle technique for the beef quality evaluation, a temporal history of speckle patterns viz. inertia moment was used as speckle activity to assess the effects of the laser incident angle, laser wavelength, and lighting intensity on beef dynamic biospeckle quality. The single factor experimental design was firstly applied to determine preliminary suitable lighting conditions for the later Box-Behnken experimental design. Subsequently, a response surface regression function of three lighting factors was obtained to optimize the measurement conditions for beef dynamic biospeckle. The results demonstrated that the speckle activity could reach 476.04, the determination coefficient R^2 was 0.992, root mean square error was 8.14, bias factor (B_f) and accuracy factor (A_f) values were within the acceptable range of $1.0 < B_f < A_f < 1.05$ via the optimal processing. Therefore, for the further beef biospeckle measurement, the lighting conditions were as follows: lighting intensity was 30 mW, laser wavelength was 635 nm and laser incident angle was 15°. In conclusion, the analysis of different lighting factors for the biospeckle acquisition might improve the qualitative or quantificational identification accuracy of beef dynamic biospeckle, and it also provides theoretical reference for the biospeckle measurement of other foods.

Key words: beef; laser speckle; speckle activity; rapid detection; condition optimization

0 Introduction

As development of economy and optimization of consumption structure, consumption of beef got rapid growth in China[1]. Therefore, more attention has been put on beef quality by meat industry, and it was usually evaluated by expert judgment and mechanical equipment. The expert judgment could ensure lower misclassifications and non-destructive grading process, but it might induce inconsistent results by different persons[2]. Meanwhile, the mechanical equipment could be an option to estimate meat quality; However, the problems existed in these tests are that they are time consuming, costly and destructive[3]. The dynamic laser speckle is a portable, non-invasive and low-cost technique, which has been widely used in agricultural products[4-5]. Nonetheless, the determination of relevant factors in the process of analysis and optimization is required to be carried out. To optimize the measurement conditions of dynamic laser speckle technique for the beef quality evaluation, a temporal history of speckle patterns was used as speckle activity to assess the effects of the laser incident angle, laser wavelength, and lighting intensity on beef dynamic biospeckle quality.

1 Materials and methods

1.1 Materials preparation

A total of thirty beef slices from the same anatomical locations (*longissimus dorsi*) were prepared manually, and meat slices were approximately trimmed to the size of 6 cm × 6 cm × 3 cm[6] by a meat cutting knife. Sterilizing treatment was conducted by employing 1% lactic acid[7]. The beef samples were vacuum packed

Received date: 2015-05-14 Accepted date: 2015-06-24
Supported by National Natural Science Foundation of China (Grant No. 31271896)
Corresponding author: Dong Qingli, associate Professor. E-mail: Dongqingli@126.com. Tel: +86-13585971239.

and aged under 4℃[8].

1.2 Biospeckle imaging system and image acquisition

A laboratory biospeckle imaging system was used to acquire images of the samples[8]. The system was comprised an illumination chamber, a COMS camera equipped with focal length of 8 mm, and a He-Ne laser generator. Each biospeckle movie was recorded by the camera with 640 × 486 resolutions for 4 s at imaging speed of 15 frames per second. The whole system was enclosed by a dark wooden chamber to avoid any stray light from the surrounding environment.

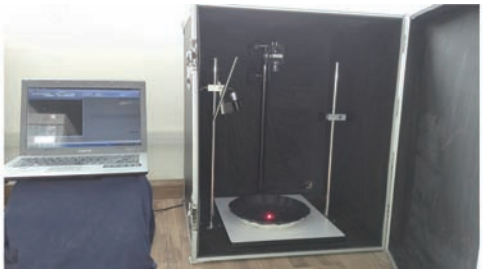

Fig. 1 Picture of dynamic laser speckle imaging system

1.3 Single factor and response surface experiment design

The temporal history of speckle patterns were chosen as the evaluation parameter, and the laser incident angle, laser wavelength and light intensity were studied to measure the precision of beef aging process.

Experiment 1: the laser incident angle was fixed at 30° and laser wavelength was set at 635 nm, and the images were captured at 5 mW, 10 mW, 20 mW, 30 mW, 50 mW and 80 mW.

Experiment 2: the laser incident angle was fixed at 30°, light intensity was set at 30 mW, and the images were captured at 405 nm, 520 nm, 635 nm and 780 nm.

Experiment 3: the light intensity was fixed at 30 mW, laser wavelength was set at 635 nm, and the images were captured at 15°, 30°, 45° and 60°.

According to the results of single factor experiments, response surface optimization was designed by Box-Behnken experiment as shown in Tab. 1, the details of the response surface optimization was listed in Tab. 2. Stepwise regression method was used with entering and withdrawing levels of 0.05 and 0.10, respectively. Totally 17 sets of data of different light intensities, light wavelengths and light incident angles were used to establish the response surface model (RSM).

Tab. 1 Factors and levels of Box-Behnken design

Levels	Factors		
	Light intensity A/mW	Laser wavelength B/nm	Laser incident angle C/(°)
−1	10	405	15
0	20	520	30
1	30	635	45

1.4 Calculation of speckle activity

For every state of the phenomenon being assessed, totally 382 successive images of the dynamical speckle pattern were registered and a certain column was selected among them. With that column, a new composite image was then developed, which was named as temporal history of speckle patterns (THSP)[9]. Inertia moment (IM) was based on occurrence of successive pixels intensity values from a temporal history of speckle patterns to generate the number and quantify speckle activity. A co-occurrence matrix[10] was used by IM to store the number of occurrences of a grey scale intensity i, which was followed in the next time by a grey scale intensity j. One of the 382 images and THSP with high and low speckle activities were shown in Fig. 2. The speckle activity was quantified by IM as follows[11]

$$C_{OM} = [N_{ij}] \tag{1}$$

$$M_{ij} = N_{ij} / \sum_{j} N_{ij} \tag{2}$$

$$I_M = \sum_{ij} M_{ij}(i-j)^2 \tag{3}$$

where C_{OM} presents the co-occurrence matrix, and I_M presents the speckle activity. N_{ij} is the occurrences of a certain valve i followed in the next time step by a value j. M_{ij} is the normalized of COM.

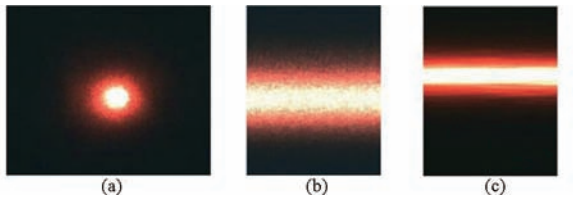

Fig. 2 Random intercept frame in video and temporal history of speckle patterns (a. one of the 382 images; b. samples with high speckle activity; c. samples with low speckle activity)

2 Results

2.1 Effect of light intensity on beef dynamic biospeckle imaging

In Experiment 1, the changes of speckle activity during the aging of beef were plotted in Fig. 3. A trend

of decrease with the increase of time was performed. During the time of 3 ~ 5 d and 5 ~ 7 d, the reduction was large, and after 7 d the column gradually tended to be stable and had a small rising. There were some slight discrepancies with the results of Amaral[12], which might be due to the breed of cattle used in different studies. Moreover, a trend of decrease after increase was presented with the increase of light intensity, and this was similar with the study of Yu[13]. When light intensity was 10 mW, 20 mW and 30 mW, speckle activity was significantly higher than that under other conditions ($P < 0.05$). Therefore, 10 mW, 20 mW and 30 mW were chosen in the Box-Behnken response surface experiment.

Change of speckle activity along with time might due to the changes of beef occurred in the process of aging. This process mainly ended during 7 ~ 10 d[14], then the quality of beef would stay stable. While the light intensity was too low, the speckle image information was partially missed, the image contrast might be low; light intensity increased with the speckle activity increased until light intensity reached supersaturation.

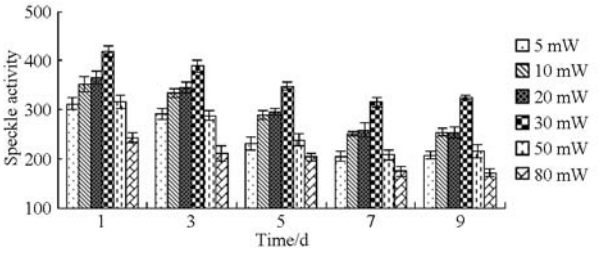

Fig. 3 Effects of lighting intensity on the speckle activity of beef speckle

2.2 Effect of laser wavelength on beef dynamic biospeckle imaging

The result of Experiment 2 for speckle activity changes during the aging of beef showed that with the increase of time, speckle activity decreased (Fig. 4). The magnitude of decreases during 3 ~ 7 d was obvious, and then it turned to be stable during 7 ~ 9 d. Furthermore, a trend of decreases after increases was presented. The maximum value appeared at wavelength of 635 nm, which was the same with the most commonly used wavelength[15]. The speckle activities at wavelengths of 405 nm, 520 nm and 635 nm, were significantly higher than that at 780 nm ($P < 0.05$). Therefore, 405 nm, 520 nm and 635 nm were chosen in the Box-Behnken response surface experiment.

The change trend of speckle activity along with the change of laser wavelength might be associated with the colour of the beef. When the laser colour was similar with the sample, scattering mode would be the main one[14]. It was usually regarded that the red light speckle had higher activity than red and green light speckles. In addition, the wavelength of 780 nm was between the visible and near-infrared lights, which emitted light too weak to be captured by camera.

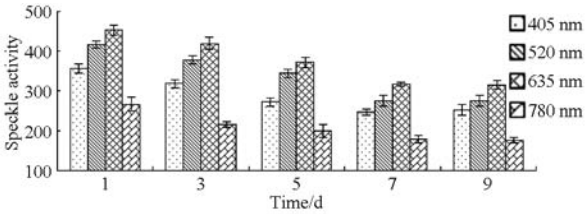

Fig. 4 Effects of laser wavelength on speckle activity of beef speckle

2.3 Effect of laser wavelength on beef dynamic biospeckle imaging

In Experiment 3, speckle activity changes during the aging of beef were shown in Fig. 5. Speckle activity was decreased with the increase of time, and showed to be stable during 7 ~ 9 d. A trend of decrease after increase appeared with the increase of incident angle. Besides, when the incident angle was 30°, speckle activity reached maximum. The speckle activities of 15°, 30° and 45° were higher than that of 60° ($P < 0.5$). Thereby, 15°, 30° and 45° were chosen in the Box-Behnken response surface experiment.

With the increase of incident angle, the light reflected into the camera would be decreased gradually, and the light intensity was abated. In addition, different colours of light had different proportions of scattering and reflection[16], thus the speckle activity was increased and then decreased, instead of reduction merely.

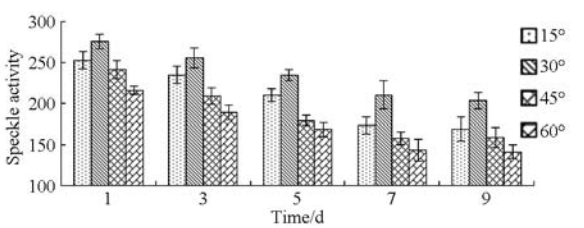

Fig. 5 Effects of laser incident angle on speckle activity of beef speckle

2.4 Results of response surface optimization

Results of response surface were shown in Tab. 2,

the response surface model (RSM) was established by speckle activity factors of light intensity (A), laser wavelength (B) and incident angle (C), which were as follows

$$Y = 2\,380.70 + 2.00A - 8.71B - 19.21C - 0.09AC + 0.14A^2 + 8.76 \times 10^{-3}B^2 + 0.09C^2 \quad (4)$$

where Y is the value of speckle activity.

The analysis of variance (ANOVA) demonstrated that model coefficient was significant ($P < 0.05$), while lack of fit was not significant ($P > 0.05$). The results suggested that RSM could simulate the effect of factors of light intensity, laser wavelength and incident angle on speckle activity ($R^2 = 0.992$). In addition, A, B, C, and interaction effect of A and C all had significant effect on the model.

The interaction effect of A and C was shown in Fig. 6. The results indicated that the interaction effect of A and C on speckle activity was significant. It could be seen that the optimal conditions of light intensity, laser wavelength and light incident angle were 30 mW, 635 nm and 15° as speckle activity was kept at the highest level.

Tab. 2 Design and results of Box-Behnken experiment

Tests No.	A	B	C	Speckle activity (mean ± SD)
1	10	520	45	166.79 ± 7.81[a]
2	10	520	15	180.39 ± 3.45[ab]
3 *	20	520	30	189.01 ± 7.77[b]
4 *	20	520	30	192.23 ± 5.82[b]
5 *	20	520	30	194.06 ± 12.31[b]
6 *	20	520	30	196.43 ± 9.23[b]
7 *	20	520	30	205.48 ± 4.49[b]
8	10	405	30	242.94 ± 6.11[c]
9	30	520	45	255.32 ± 7.91[cd]
10	20	405	45	273.49 ± 9.23[d]
11	20	405	15	296.78 ± 14.41[e]
12	10	635	30	316.09 ± 2.42[ef]
13	30	405	30	319.76 ± 7.67[f]
14	30	520	15	320.97 ± 22.75[f]
15	20	635	45	351.55 ± 10.27[g]
16	20	635	15	403.60 ± 6.93[h]
17	30	635	30	424.01 ± 8.88[i]

* Levels were centrals of the test; column with different lowercase superscripts had significant differences ($P < 0.05$).

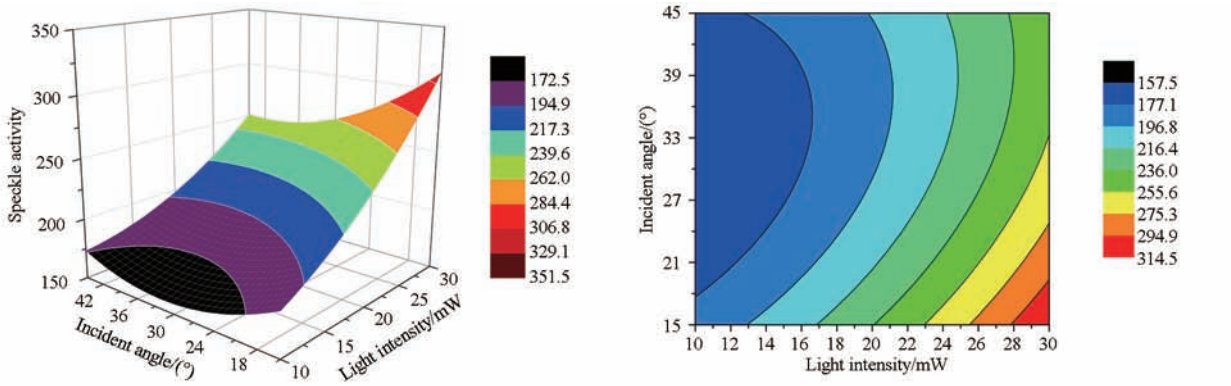

Fig. 6 Response surface and contour for inhibition zones of light intensity and laser incident angle

The established RSM was evaluated by 15 treatments as shown in Tab. 3 and Tab. 4, respectively, which were selected randomly from Tab. 2 and in wide range. The root mean square error was 8.14, accurate factor (A_f) and bias factor (B_f) were $1.0 < B_f < A_f < 1.05$[17], which belonged to the acceptable range. Results showed that the regression prediction equation had high reliability.

3 Conclusions

Through the study of different aging degrees of beef, it could be seen that light intensity, laser wavelength and incident angle had great influence on speckle activity. The results of Box-Behnken design experiment indicated that there was a significant interaction effect between the light intensity and incident angle. According to the mathematical validation, the RSM for predicting speckle activity had high reliability ($R^2 = 0.992$). When the light intensity was 30 mW, laser wavelength was 635 nm, and the incident angle was 15°, the speckle activity reached the maximum value of 476.04. By reasonable selection of dynamic laser speckle measurement conditions, the research provided reference for improving the recognition accuracy of speckle activity.

Tab. 3 Observed and predicted inhibition zones toward speckle activity by RSM at different light intensities, laser wavelengths and laser incident angles

Tests No.	Light intensity/mW	Laser wavelength/nm	Incident angle/(°)	Speckle activity	
				Observations	Predictions
1	10	520	45	166.79	173.28
2	10	405	30	242.94	228.23
3	10	635	30	316.09	319.70
4*	20	520	30	205.48	195.44
5*	20	520	30	189.01	195.44
6*	20	520	30	192.23	195.44
7	20	405	15	296.78	305.39
8	30	405	30	319.76	331.70
9	30	520	45	255.32	250.71
10	30	635	30	424.01	423.17

Tab. 4 Observed and predicted inhibition zones for validation toward speckle activity by RSM at different light intensities, wavelengths and light incident angles

Tests No.	Light intensity/mW	Laser wavelength/nm	Incident angle/(°)	Speckle activity	
				Observations	Predictions
1	10	520	45	170.03	173.28
2	20	520	30	203.34	195.44
3	20	635	15	383.51	396.86
4	20	405	45	260.59	267.64
5	30	635	45	419.40	423.17

References

[1] Desmond E M, Kenny T A, Ward P, et al. Effect of rapid and conventional cooling methods on the quality of cooked ham joints[J]. Meat Science, 2000,56(3): 271 – 277.

[2] Jackman P, Sun D W, Allen P. Resent advances in the use of computer vision technology in the quality assessment of fresh meat [J]. Food Science & Technology, 2011,22(4): 185 – 197.

[3] Zhang Haiyun, Peng Yankun, Wang Wei, et al. Nondestructive real time detection system for assessing main quality parameters of fresh pork[J]. Transactions of the Chinese Society for Agricultural Machinery, 2013, 44(4): 146 – 151.

[4] Kenny E, Coakley D, Boyle G. Non-contact in vivo measurement of ocular microtremor using laser speckle correlation metrology [J]. Physiological Measurement, 2014,35(7): 1229 – 1243.

[5] Liu Shanmei, Li Xiaoyu, Zhong Xiongben, et al. Nondestructive detection of water content in fresh pork based on hyerspectral imaging technology [J]. Transactions of the Chinese Society for Agricultural Machinery, 2013,44(Supp. 1): 165 – 171.

[6] Brabin D F, Valous N A, Sun D W. Tenderness prediction in porcine *longissimus dorsi* muscles using instrumental measurements along with NIR hyperspectral and computer vision imagery [J]. Innovative Food Science and Emerging Technologies. 2013, 20: 335 – 342.

[7] Kamruzzaman M, Elmasry g, Sun D W, et al. Non-destructive assessment of instrumental and sensory tenderness of lamb meat using NIR hyperspectral imaging [J]. Food Chemistry,2013,141(1): 389 ~ 396.

[8] Hu Menghan, Dong Qingli. A kind of general visual test bench of food analysis: China 201220059147.4 [P]. 2012-02-22.

[9] Braga R A, Fabbro I D, Borem F M, et al. Assessment of seed viability by laser speckle techniques [J]. Biosystems Engineering, 2003, 86(3): 287 – 294.

[10] Hu Menghan, Dong Qingli, Liu Baolin, et al. Color and texture monitoring based on computer vision during banana storage[J]. Transactions of the Chinese Society for Agricultural Machinery, 2013,44(8): 180 – 184.

[11] Arizaga R, Trivi M, Rabal H. Speckle time evolution characterization by the co-occurrence matrix analysis [J]. Optics and Laser Technology, 1999,31(2): 163 – 169.

[12] Amaral I C, Braga R A, Ramos E M, et al. Application of speckle laser technique for determining biological phenomena related to beef aging[J]. Journal of Food Engineering, 2013,119(1): 135 – 139.

[13] Yu Zhiyang, Liu Zhijian. Factors influencing laser speckle in surface roughness measurement[J]. Journal of Heilongjiang University of Science and Technology, 2010,20(6): 460 – 462.

[14] Gao Xue, Xu Shangzhong, Zhang Yinghan, et al. Factors affecting beef quality after Slaughter[J]. Journal of Yellow Cattle Science, 2004,30(1): 26 – 29.

[15] Zdunek A, Adamiak A, Pieczywek P. The speckle method for the investigation of agricultural crops: a review[J]. Optics and Lasers in Engineering, 2014, 52: 276 – 285.

[16] Briers J. Wavelength dependence of intensity fluctuations in laser speckle patterns from biological specimens[J]. Optics Communications, 1975,13(3): 324 – 326.

[17] Ye K, Wang H H, Zhang X X, et al. Development and validation of a molecular predictive model to describe the growth of *Listeria monocytogenes* in vacuum-packaged chilled pork[J]. Food Control, 2013,32(1): 246 – 254.

doi:10.6041/j.issn.1000-1298.2016.02.038

牛肉激光动态散斑活性影响因素研究

董庆利　金　曼　胡孟晗　刘宝林
（上海理工大学医疗器械与食品学院，上海 200093）

摘要：以时间序列散斑图的惯性力矩作为散斑活性，研究新鲜牛肉图像散斑活性的相关影响因素，以优化激光散斑的测定效果。采用 He－Ne 激光器照射牛肉表面，通过工业相机获取图像，测得时间序列散斑图的散斑活性值，检测成像时图像的精度差异，研究不同条件下牛肉散斑活性的变化趋势。应用 Box－Behnken 试验设计，建立光照强度、激光波长和入射角度 3 个因素的二次多项式回归模型并进行分析。结果表明光照强度、激光波长和入射角度对牛肉散斑活性影响显著，得到牛肉图像散斑活性值最大时的优化测定条件为激光波长 635 nm、光照强度 30 mW、入射角度 15°，在此条件下，散斑图像的散斑活性达到 476.04，散斑活性预测模型的决定系数 R^2 为 0.992，均方根误差 R_{MSE} 为 8.14，偏差因子（B_f）和准确因子（A_f）均在可接受范围内。明确不同因素对新鲜牛肉激光动态散斑图像的影响，可提高激光动态散斑活性的识别精度，为改进牛肉品质的测定方法提供了理论依据。

关键词：牛肉；激光散斑；散斑活性；快速检测；条件优化
中图分类号：TS251.5⁺2；O432.1⁺2　　**文献标识码**：A　　**文章编号**：1000-1298(2016)02-0288-07

Factors Affecting Dynamic Laser Speckle Activity of Beef

Dong Qingli　Jin Man　Hu Menghan　Liu Baolin
(*School of Medical Instrument and Food Engineering*,
University of Shanghai for Science and Technology, *Shanghai* 200093, *China*)

Abstract: Dynamic laser speckle technique, also termed as dynamic biospeckle, is a portable and non-invasive as well as low-cost screening tool for online or point-of-sale applications on agricultural products. A custom made dynamic laser speckle system mainly consisted of a He－Ne laser generator operating at the four wavelengths of 405 nm, 520 nm, 635 nm and 780 nm, respectively, an industrial CMOS camera for the sequential images acquisition, a computer and a height adjustable sample stage. The lighting and imaging units were placed into an illumination chamber to avoid the interference of natural light. In order to optimize the measurement conditions of dynamic laser speckle technique for the beef quality evaluation, a temporal history of speckle patterns *viz*. inertia moment was used as speckle activity to assess the effects of the laser incident angle, laser wavelength, and lighting intensity on beef dynamic biospeckle quality. The single factor experimental design was first applied for determining preliminary suitable lighting conditions for the later Box－Behnken experimental design. Subsequently, a response surface regression function of three lighting factors was obtained to optimize the measurement conditions for beef dynamic biospeckle. Above results demonstrated that the speckle activity could reach 476.04, the R^2 value was 0.992, root mean square error value was 8.14, bias factor (B_f) and accuracy factor (A_f) values were within the acceptable range of $1.0 < B_f < A_f < 1.05$ via the optimal processing. Therefore, for the further beef biospeckle measurement, the lighting conditions are as follows: lighting intensity is 30 mW, laser wavelength is 635 nm and laser incident angle is 15°. In a conclusion, the analysis of different lighting factors for the biospeckle acquisition might improve the qualitative or quantificational identification

收稿日期：2015－05－14　修回日期：2015－06－24
基金项目：国家自然科学基金面上项目（31271896）、上海市科委长三角科技联合攻关领域项目（15395810900）和上海市研究生创新基金项目（JWCXSL1401）
作者简介：董庆利（1979—），男，副教授，主要从事畜产品安全和质量控制研究，E-mail：dongqingli@126.com

accuracy of beef dynamic biospeckle, and also provide the theoretical reference for the biospeckle measurement of the other foods.

Key words: beef; laser speckle; speckle activity; rapid detection; condition optimization

引言

牛肉作为大众日常所需的重要食品之一，具有高蛋白质、低脂肪、高矿物质及高维生素等特点[1]，深受消费者的青睐。尤其是近年来，随着经济的发展，人民生活水平以及购买力的不断提高，我国牛肉及其制品的生产和消费总量保持持续增长。随着消费观念的改变，肉类市场需求向多样化发展，消费结构也在逐步调整优化，牛肉的消费比重得到了快速增长[2]。

新鲜牛肉的品质包括其所具有的外观、风味、营养、卫生等各种与加工和食用相关的物理与化学性状。目前，我国使用最普遍的肉类品质检验方法是人工检验法，包括感官检测法和物理检测法。感官检测方法不仅需要大量劳动力和时间，而且花费高、速度慢，对人员专业要求比较高，费时费力，评价结果也容易受到个人的主观因素影响，同时，对同一样品的检测也会因为检测者的个体差异导致结果出现偏差[3]。物理检测方法测定准确，但在测量熟肉时，对样本有一定破坏，且测量方法繁琐，需要较长时间[4]。激光散斑(Laser speckle)测量技术是一种成本较低、快速、无损、实时和可定性/定量的光学无损检测方法[5]，在生物医学和农业领域得到了广泛的应用[6-7]。许多研究利用激光照射在物体表面而产生的散斑现象[8-9]，通过抓取、处理散斑图像，将散斑的强度变化情况与农畜产品的特性相关联，从而实现农畜产品的快速检测。国外已有基于激光动态散斑对牛肉品质进行测定的研究[10]，但是对测定过程中相关因素的分析和优化尚待开展。

本文采用 He－Ne 激光器照射牛肉表面，通过工业相机获取图像，将获得的激光动态散斑视频进行处理，提取每一帧的固定列组成时间序列散斑图(Temporal history of speckles patterns)，以时间序列散斑图的参数值惯性力矩作为响应值散斑活性，对激光波长、光照强度和入射角度 3 个因素变化所得图像的散斑活性(Speckle activity)差异进行评价，研究各因素对散斑图像的影响，建立散斑活性对不同测定因素下的预测模型，探讨测定牛肉散斑活性的最优条件组合并进行优化，为改进牛肉激光动态散斑的测定方法提供理论依据。

1　材料与方法

1.1　试验材料与预处理

屠宰于 24 h 内的新鲜牛肉购于上海市当地超市，取 12 ~ 13 肋节间的背最长肌(*longissimus dorsi*)，用刀具切成 6 cm × 3 cm × 3 cm[11]的小块，用 1% 的乳酸溶液清洗消毒[12]后，用保鲜袋分别密封包装，贮存于 4℃ 冰箱中进行熟化[13]，用于后续测定。试验过程中每 2 d 对肉样进行生物散斑测定拍照，共测定 5 次。

1.2　主要设备与试验装置

DFM 72BUC02 型定焦工业相机(上海英诚图像技术有限公司)；HLM 1845 型激光发射器(广东省深圳市铂镭公司)；P428 型便携式计算机(韩国三星公司)；DZ－280/2 SE 型真空包装机(天津市绿叶公司)。

牛肉激光动态散斑图像获取系统搭建如图 1、2 所示[14]，主要由激光发射器、工业相机、计算机等组成。试验使用定焦工业相机进行散斑图像采集，相机距样品台 50 cm，激光发射器的强度调节由偏振片实现。工业相机采集图像分辨率为 640 像素 × 486 像素，焦距为 8 mm，图像获取速度为 25 帧/s，图像采集时间为 15 s，每次图像采集重复 3 次。

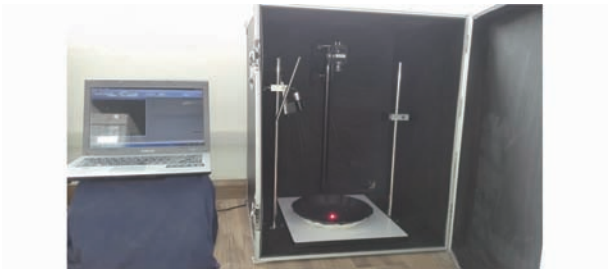

图 1　激光动态散斑成像系统实物图

Fig. 1　Picture of dynamic laser speckle imaging system

1.3　单因素试验设计

以时序散斑图的特征参数散斑活性为评价指标，分别研究激光器入射角度、激光波长与光照强度 3 个因素对牛肉熟化过程中散斑活性测定精度的影响。

测定光照强度对牛肉熟化过程中散斑活性测定精度的影响时，固定激光器入射角度为 30°，激光波长为 635 nm，在光照强度分别为 5、10、20、30、40、50、80 mW 时对牛肉样品进行图像采集。

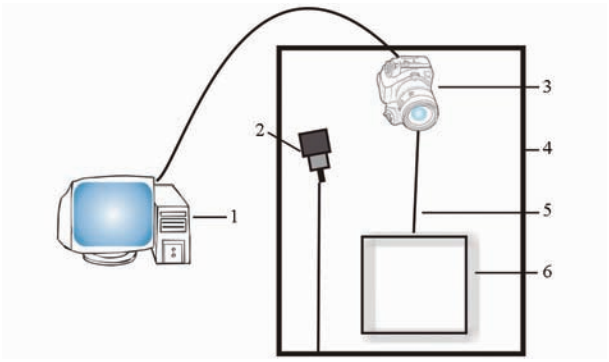

图 2 激光动态散斑成像系统示意图

Fig. 2 Diagram of dynamic laser speckle imaging system

1. 计算机 2. 激光发射器 3. 工业相机 4. 封闭箱子 5. 可升降杆 6. 样品台

测定激光波长对牛肉熟化过程中散斑活性测定精度的影响时,固定激光器光照强度为 30 mW,激光器入射角度为 30°,分别在激光波长为 405、520、635、780 nm 时对牛肉样品进行图像采集。

测定入射角度对牛肉熟化过程中散斑活性测定精度的影响时,固定激光器光照强度为 30 mW,激光波长为 635 nm,分别在入射角度为 15°、30°、45°、60°时对牛肉样品进行图像采集。

1.4 响应面优化试验设计

采用美国 Stat - Ease 公司 Design - Expert 8.0.6 软件中的 Box - Behnken 对试验进行设计(表 1),根据 1.3 节的测定结果确定各因素水平值,对激光动态散斑活性进行响应面优化,考察各因素对牛肉品质测定的最佳测定组合,具体实施如表 2 所示。应用逐步回归方法(引入水平为 0.05,去除水平为 0.10)对表 2 的 17 组数据建立散斑活性对因素光照强度、激光波长和入射角度的响应曲面模型(RSM)。

表 1 Box - Behnken 试验分析因素与水平

Tab. 1 Factors and levels of Box - Behnken design

水平	因素		
	光照强度 A/mW	激光波长 B/nm	激光入射角度 C/(°)
-1	10	405	15
0	20	520	30
1	30	635	45

1.5 回归方程的数学验证

获得显著的多元回归方程后,分别从表 2 中随机选取的 10 组处理与重新进行验证试验的 5 组处理代入方程,对模型进行验证。通过对模型的均方根误差(Root mean square error)R_{MSE}、准确因子(Accuracy factor)A_f、偏差因子(Bias factor)B_f 对模型进行评价,表达式为[15]

$$R_{MSE} = \sqrt{\frac{\sum (V_0 - V_p)^2}{n}} \tag{1}$$

$$A_f = 10^{\frac{\sum \left| \lg \frac{V_p}{V_0} \right|}{n}} \tag{2}$$

$$B_f = 10^{\frac{\sum \lg \frac{V_p}{V_0}}{n}} \tag{3}$$

式中 V_p——试验观测值 V_0——模型预测值

n——试验次数

表 2 Box - Behnken 响应面试验设计与结果

Tab. 2 Design and results of Box - Behnken experiment

试验序号	A/mW	B/mm	C/(°)	散斑活性(平均值 ± 标准差)
1	10	520	45	166.79 ± 7.81^{a}
2	10	520	15	180.39 ± 3.45^{ab}
3*	20	520	30	189.01 ± 7.77^{b}
4*	20	520	30	192.23 ± 5.82^{b}
5*	20	520	30	194.06 ± 12.31^{b}
6*	20	520	30	196.43 ± 9.23^{b}
7*	20	520	30	205.48 ± 4.49^{b}
8	10	405	30	242.94 ± 6.11^{c}
9	30	520	45	255.32 ± 7.91^{cd}
10	20	405	45	273.49 ± 9.23^{d}
11	20	405	15	296.78 ± 14.41^{e}
12	10	635	30	316.09 ± 2.42^{ef}
13	30	405	30	319.76 ± 7.67^{f}
14	30	520	15	320.97 ± 22.75^{f}
15	20	635	45	351.55 ± 10.27^{g}
16	20	635	15	403.60 ± 6.93^{h}
17	30	635	30	424.01 ± 8.88^{i}

注:* 中心点条件;同列上标不同小写字母者差异显著($P < 0.05$)。

1.6 散斑图像的处理及散斑活性的计算

应用美国 The MathWorks 公司开发的 Matlab R2014a 软件对试验所得视频进行处理,记录牛肉样品的生物散斑图像变化,使用转动惯量法(Inertia moment)对图像进行处理并计算图像的散斑活性。

1.6.1 散斑图像处理

(1)构建时间序列散斑图[16]:取所获视频中初始时刻的一帧图像的中间一列,并以此时刻为起点,将之后每一帧图像中该列的点都提取出来,并按时间顺序依次排列起来,构成一幅新的图像即为时间序列散斑图,如图 3 所示。时间序列散斑图体现了视频中光变化的剧烈程度。

(2)构建灰度共生矩阵($\boldsymbol{C}_{OM}$)[17]:对一幅时间序列散斑图来说,若元素 i(像素 i 的灰度)后面接着出现元素 j(像素 j 的灰度)的次数是 N,就把 N 这个值赋给所构建的共生矩阵中第 i 行第 j 列的元素,图 4 为计算规则示意图。

1.6.2 散斑活性的计算

散斑活性的计算基于时间序列散斑图和灰度共生矩阵的构建,通过灰度共生矩阵 $\boldsymbol{C}_{OM}$ 可计算每个元素组合 N_{ij} 出现的概率 M_{ij}。利用 $M_{ij}^2(i-j)$ 得到

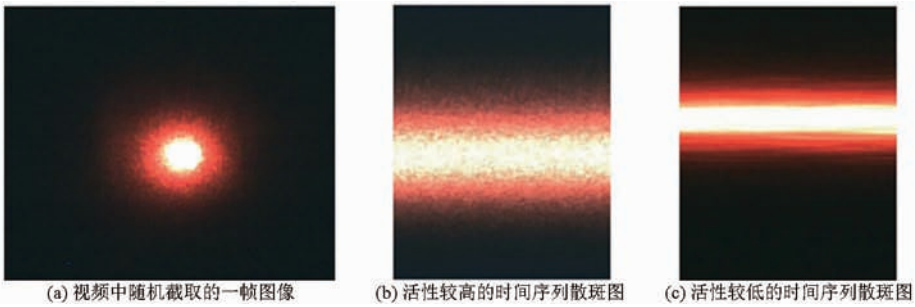

图 3　视频中随机截取的一帧图像及时间序列散斑图

Fig. 3　Random intercept frame in video and temporal history of speckles patterns

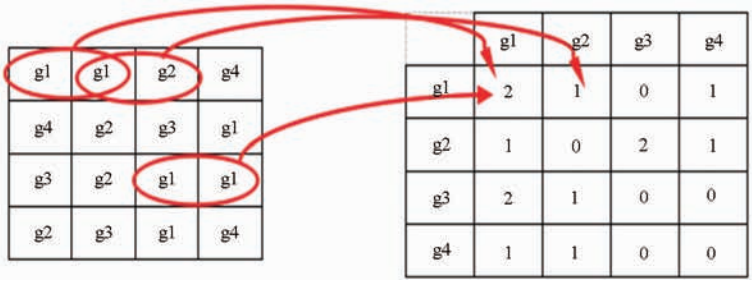

图 4　灰度共生矩阵的计算规则

Fig. 4　Calculation rule of gray-level co-occurrence matrix

元素偏离主对角线的程度(当 i 等于 j 时偏离程度为零),I_M 为所有非零元素偏离主对角线的程度即为散斑活性,具体计算公式为[18]

$$\boldsymbol{C}_{OM} = [N_{ij}] \tag{4}$$

$$M_{ij} = N_{ij} / \sum_{j} N_{ij} \tag{5}$$

$$I_M = \sum_{ij} M_{ij}^2 (i-j) \tag{6}$$

1.7　数据处理与统计分析

研究中涉及的数据处理与统计分析在由北京金山办公软件有限公司和珠海金山办公软件公司开发的软件 WPS Office 9.1.0.4984 中进行。文中的平均数均为算术平均数,标准差均为给定样品的标准偏差。方差分析运用最小显著差异法(Least significant difference, LSD)进行均值多重比较,在 IBM 公司开发的 SPSS Statistic 17.0 中进行。响应面图与等高线图的绘制在美国 OriginLab 开发的 Origin 8.5 中进行。

2　试验与结果分析

2.1　光照强度对牛肉激光动态散斑成像的影响

激光器入射角度为 30°,激光波长为 635 nm,在光照强度分别为 5、10、20、30、50、80 mW 时,绘制牛肉熟化过程中的散斑活性如图 5 所示,可以看出随着时间的增加,散斑活性逐渐减小,且在 3 ~ 5 d 和 5 ~ 7 d 时减小的幅度较大,在 7 d 以后逐渐趋于稳定并有小幅升高,此结果与 Amaral 等[10] 的研究结果略有差异,可能与牛的品种差异有关。随着光照强度增大,散斑活性值呈先增大后减小的趋势且在 30 mW 时达到最大值,这与于智洋等[19] 的研究结果一致。光照强度在 10、20、30 mW 时,散斑活性显著高于其他条件($P < 0.05$)。因此,在进行 Box - Behnken 响应面试验设计时,光照强度这一因素选择水平 10、20、30 mW。

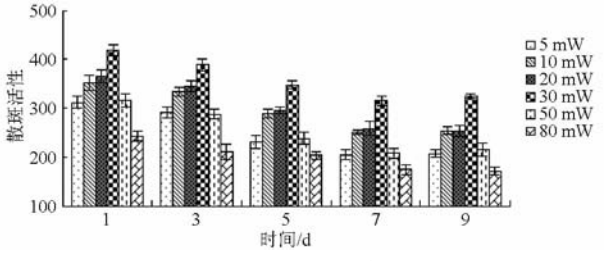

图 5　不同光照强度对牛肉图像散斑活性的影响

Fig. 5　Effects of lighting intensity on speckle analysis of beef speckle

散斑活性随时间的变化,可能是由于牛肉在贮存过程中发生排酸熟化,这一过程主要在 7 ~ 10 d 完成[20],随后品质趋于稳定。散斑活性随光照强度的变化可能是由于光照强度过低时,得到的散斑图像信息不够细致,导致图像对比度较低;而随着光照强度的增大,获得散斑活性增加;继续增大光照强度,达到过饱和状态,影响了散斑活性的变化,致使散斑活性反而下降。

2.2　激光波长对牛肉激光动态散斑成像的影响

激光器光照强度为 30 mW,入射角度为 30°,在激光波长为 405、520、635、780 nm 时,绘制牛肉熟化过程中的散斑活性如图 6 所示,可以看出随着时间

的增加,散斑活性在 3 ~ 7 d 减小较明显,在 7 ~ 9 d 时趋于稳定。随着激光波长的增加,散斑活性先增大后减小,且在波长为 635 nm 时,散斑活性值达到最大,这与激光散斑研究中最常用的波长一致[21]。光照波长为 405、520、635 nm 时散斑活性显著高于波长为 780 nm 时($P < 0.05$)。因此,在进行 Box - Behnken 响应面试验设计时,激光波长这一因素选择水平 405、520、635 nm。

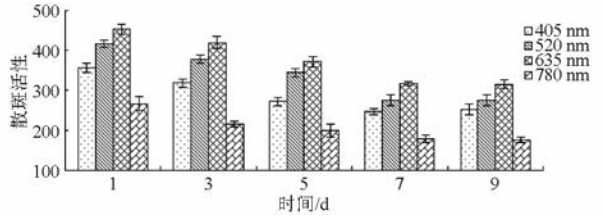

图 6 不同激光波长对牛肉图像散斑活性的影响

Fig. 6 Effects of laser wavelength on speckle analysis of beef speckle

散斑活性随激光波长的变化趋势可能是由于牛肉的颜色主要是红色,而激光颜色和待测物品颜色相同时,照射后主要以散射为主[20]。这一原因导致和牛肉颜色最接近的红光所得散斑活性最高,而绿光和蓝光相对红光所得散斑活性相对减小。此外,波长在 780 nm 时,激光处于可见光和近红外光之间,发射出的光与其他几种相比较弱,使相机难以捕捉,这种情况导致拍摄的散斑活性偏低,而其他几种光所拍摄散斑图像的活性则显著高于 780 nm 时拍摄的图像。

2.3 入射角度对牛肉激光动态散斑成像的影响

激光器光照强度为 30 mW,激光波长为 635 nm,在入射角度为 15°、30°、45°、60°时,绘制牛肉熟化过程中的散斑活性如图 7 所示。可以看出随时间增加,散斑活性逐渐减小,且在 7 ~ 9 d 时趋于稳定。随入射角度增大,散斑活性同样先增大后减小,且在入射角度为 30°时,散斑活性达到最大。入射角度为 15°、30°、45°时散斑活性显著高于入射角度为 60°时($P < 0.05$)。因此,在进行 Box - Behnken 响应面试验设计时,入射角度这一因素选择了水平 15°、30°、45°。

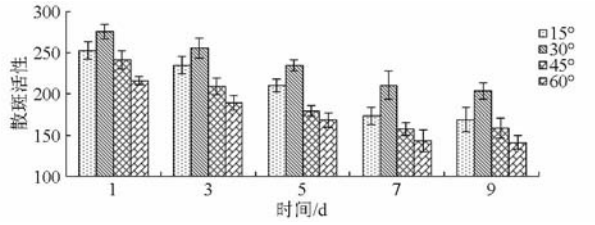

图 7 不同光源入射角度对牛肉图像散斑活性的影响

Fig. 7 Effects of laser incident angle on speckle analysis of beef speckle

散斑活性随入射角度的变化趋势可能是由于角度较小时,有更多的光通过反射进入相机,角度增大时,进入相机的光会逐渐减少,导致光强减弱,影响图像的拍摄结果。此外,光在传播过程中发生散射,是影响激光动态散斑成像的重要因素,不同颜色的光发生散射和反射的比例不同[22],导致散斑活性并非单纯减小,而是先增大后减小。

2.4 响应面优化试验结果

响应面试验结果见表 2,对表 2 中 17 组数据的响应值(散斑活性)应用逐步回归方法,建立散斑活性对因素光照强度 A、激光波长 B 与入射角度 C 的响应曲面模型为

$$Y = 2\,380.70 + 2.00A - 8.71B - 19.21C - 0.09AC + 0.14A^2 + 8.76 \times 10^{-3}B^2 + 0.09C^2 \quad (7)$$

式中 Y——散斑活性响应值

对建立的响应面模型进行方差分析显示,模型系数显著($P < 0.05$),失拟检验不显著($P > 0.05$),表明建立的响应面模型能较好模拟因素光照强度、激光波长和入射角度对散斑活性的影响(R^2 为 0.992)。对模型进行方差分析可知,除 A、B、C 外,A 与 C 的交互效应对模型也具有显著影响。

光照强度 A 与入射角度 C 对散斑活性的交互影响见图 8,表明等高线曲率较小,形状近似椭圆,

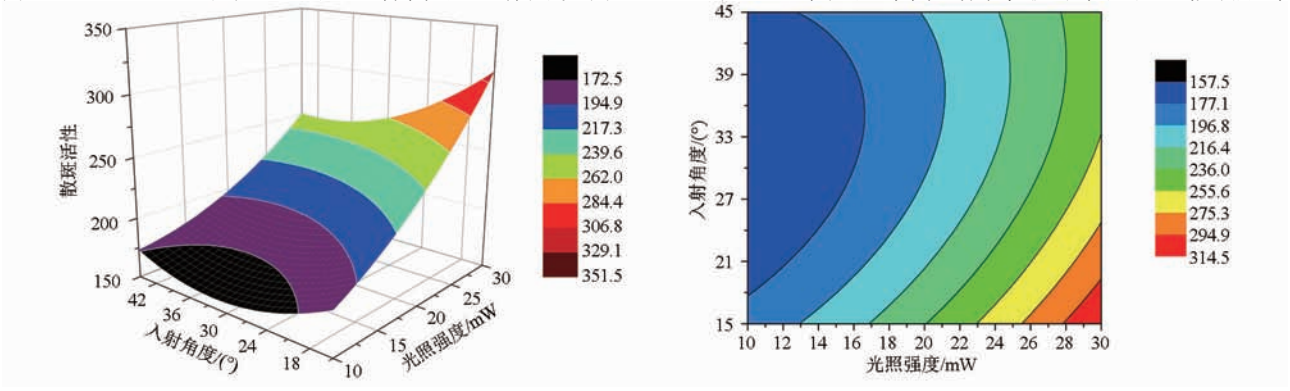

图 8 光照强度与入射角度交互效应对散斑活性的响应面图与等高线图

Fig. 8 Response surface and contour for inhibition zones of lighting intensity and laser incident angle

说明 A 与 C 交互效应对散斑活性的影响显著。当光照强度趋近于 30 mW，随着入射角度的增大，散斑活性逐渐减小。使散斑活性保持在最高水平，由此通过优化得到最优条件为：光照强度 30 mW，激光波长 635 nm，入射角度 15°，散斑活性达到 476.04。

应用建立的 RSM 回归预测方程分别对表 2 中随机选择的 10 组处理（表 3）和重新进行随机试验所得 5 组处理（表 4）进行验证，基于不同的数学检验参数得到模型的 R_{MSE} 为 8.14，小于测定值的 5%，在可接受范围内；准确因子和偏差因子为 $1.0 < B_f < A_f < 1.05$[23]，属于可接受范围。结果说明此回归预测方程可靠性较高，能够较好地预测在本试验条件下不同光照强度、激光波长和入射角度对散斑活性的影响。

表 3　不同光照强度、激光波长和入射角度时散斑活性影响的观测值与预测值

Tab. 3　Observed and predicted inhibition zones toward speckle analysis by RSM on different lighting intensities, laser wavelengths and laser incident angles

处理组	光照强度/mW	激光波长/nm	入射角度/(°)	散斑活性	
				观测值	预测值
1	10	520	45	166.79	173.28
2	10	405	30	242.94	228.23
3	10	635	30	316.09	319.70
4*	20	520	30	205.48	195.44
5*	20	520	30	189.01	195.44
6*	20	520	30	192.23	195.44
7	20	405	15	296.78	305.39
8	30	405	30	319.76	331.70
9	30	520	45	255.32	250.71
10	30	635	30	424.01	423.17

注：* 中心点条件；表中观测值为试验实际获得图像计算所得，预测值为将相应水平值代入散斑活性 RSM 回归预测模型所得，下同。

表 4　不同光照强度、激光波长和入射角度用于验证所得散斑活性影响的观测值与预测值

Tab. 4　Observed and predicted inhibition zones for validation toward speckle analysis by RSM on different illumination intensities, laser wavelengths and light incident angles

处理组	光照强度/mW	激光波长/nm	入射角度/(°)	散斑活性	
				观测值	预测值
1	10	520	45	170.03	173.28
2	20	520	30	203.34	195.44
3	20	635	15	383.51	396.86
4	20	405	45	260.59	267.64
5	30	635	45	419.40	423.17

3　讨论

3.1　散斑活性的计算方法

本研究中采用转动惯量法表征散斑活性，使不同因素条件下，不同熟化程度的牛肉样品得到很好识别，结果较好。Oulamara 等[24]在时间序列散斑图的基础上应用了转动惯量法对散斑活性进行描述，表明这种方法简单有效并可定量表征激光动态散斑随时间的变化。同时，时间序列散斑图可以较好地反映出生物活性的变化，图像的稳定性与生物活性密切相关[25]。转动惯量法还用于种子活性的测定[26]、农作物灌溉控制[27]等研究中，均表现出较可靠的测定潜力。但转动惯量法处理数据量较大[28]，已有学者将新的算法引入到激光动态散斑图像处理中，例如 Cardoso 等[29]引入了小波熵（Wavelets based entropy）和互谱（Cross-spectrum），Rabelo 等[30]提出卷积与傅里叶变换等，从而克服了处理大量数据的局限性。

3.2　牛肉样品的激光测定方法

牛肉在熟化过程中，由于乳酸的增多，牛肉中的部分蛋白质被溶出，结缔组织也被软化，从而使宰后发生僵直的牛肉变软[31]。在此过程中，牛肉细胞发生变化，持水力增加，激光照射在不同的牛肉样品表面后，出现不同的光路，使其形成的动态散斑存在差异，给激光动态散斑对牛肉品质的测定提供了基础。这一理论与 Zdunek 等[20]的观点一致，认为生物散斑的变化来源之一为细胞的变化。

研究中为使样品更加均一，采用牛同一部位的肉作为样品，修切成相同大小，并用乳酸进行消毒，独立真空包装后，进行后续测定。而在实际生产中，并不会对牛肉进行如此细致的均一处理，从而限制了实际生产应用的广泛推广。此外，牛肉的构成较为复杂，而牛肉的品质受很多因素的影响[32]，对品质的测定需要多种指标，使用单一的测定方法并不全面。所以，牛肉无损检测的发展方向之一是将两种或多种检测技术进行相互融合，从而达到快速、准确、全面地检测牛肉品质的目的。

4　结束语

通过对不同熟化程度的牛肉进行研究，并对其散斑活性进行分析，表明光照强度、激光波长及入射角度的改变对激光动态散斑具有较大的影响。通过 Box－Behnken 试验设计，表明光照强度与入射角度之间的交互效应显著。综合数学检验结果，可知散斑活性的 RSM 预测回归模型（R^2 为 0.992）可靠性较高。当光照强度为 30 mW，激光波长为 635 nm，入射角度为 15°时，散斑活性达到最大值 476.04，为合理选择激光动态散斑测定条件，提高散斑活性识别精度提供了参考。

参 考 文 献

1 田潇瑜,徐阳,彭彦昆,等.基于光谱技术的牛肉多品质参数快速检测模型[J]. 农业机械学报,2014,45(增刊):171 - 176.
Tian Xiaoyu, Xu Yang, Peng Yankun, et al. Papid detection model of beef quality based on spectroscopy[J]. Transactions of the Chinese Society for Agricultural Machinery, 2014,45(Supp.): 171 - 176. (in Chinese)

2 Desmond E M, Kenny T A, Ward P, et al. Effect of rapid and conventional cooling methods on the quality of cooked ham joints [J]. Meat Science, 2000,56(3): 271 - 277.

3 Jackman P, Sun D W, Allen P. Resent advances in the use of computer vision technology in the quality assessment of fresh meat [J]. Food Science & Technology, 2011,22(4): 185 - 197.

4 张海云,彭彦昆,王伟,等.生鲜猪肉主要品质参数无损在线检测系统[J]. 农业机械学报,2013,44(4):146 - 151.
Zhang Haiyun, Peng Yankun, Wang Wei, et al. Nondestructive real time detection system for assessing main quality parameters of fresh pork[J]. Transactions of the Chinese Society for Agricultural Machinery, 2013,44(4): 146 - 151. (in Chinese)

5 胡孟晗,董庆利,刘宝林,等.生物散斑技术在农产品品质分析中的应用[J]. 农业工程学报,2013,29(24):284 - 292.
Hu Menghan, Dong Qingli, Liu Baolin, et al. Application of biospeckle on analysis of agricultural products quality [J]. Transactions of the CSAE, 2013, 29(24): 284 - 292. (in Chinese)

6 Kenny E, Coakley D, Boyle G. Non-contact in vivo measurement of ocular microtremor using laser speckle correlation metrology [J]. Physiological Measurement, 2014,35(7): 1229 - 1243.

7 Rodriguez M H. State of the art in farm animal sperm evaluation[J]. Reproduction Fertility and Development, 2007,19(1): 91 - 101.

8 Cardoso R R, Braga R A. Enhancement of the robustness on dynamic speckle laser numerical analysis[J]. Optics and Lasers in Engineering, 2014,63: 19 - 24.

9 许德毓,蔡小舒.激光散射法测量 TSP 和 PM10 的最佳采光角及立体角的研究[J]. 上海理工大学学报,2001,23(1):57 - 65.
Xu Deyu, Cai Xiaoshu. A theoretical study on light scattering method for measuring TSP and PM10[J]. Journal of University of Shanghai for Science and Technology, 2001, 23(1): 57 - 65. (in Chinese)

10 Amaral I C, Braga R A, Ramos E M, et al. Application of speckle laser technique for determining biological phenomena related to beef aging[J]. Journal of Food Engineering, 2013,119(1): 135 - 139.

11 刘善梅,李小昱,钟雄斌,等.基于高光谱成像技术的生鲜猪肉含水率无损检测[J]. 农业机械学报,2013,44(增刊 1): 165 - 171.
Liu Shanmei, Li Xiaoyu, Zhong Xiongbin, et al. Non-destructive detection of water content in fresh pork based on hyerspectral imaging technology[J]. Transactions of the Chinese Society for Agricultural Machinery, 2013,44(Supp. 1): 165 - 171. (in Chinese)

12 Brabin D F, Valous N A, Sun D W. Tenderness prediction in porcine longissimus dorsi muscles using instrumental measurements along with NIR hyperspectral and computer vision imagery[J]. Innovative Food Science and Emerging Technologies, 2013,20: 335 - 342.

13 Kamruzzaman M, Elmasry G, Sun D W, et al. Non-destructive assessment of instrumental and sensory tenderness of lamb meat using NIR hyperspectral imaging[J]. Food Chemistry,2013,141(1): 389 - 396.

14 胡孟晗,董庆利.一种食品分析通用型视觉实验台:中国,201220059147.4[P]. 2012 - 02 - 22.

15 董庆利,李保国,蔡佳彦,等.冷藏温度下乳酸菌饮料中乳酸菌失活模型的建立[J]. 中国乳品工业,2009,37(5): 6 - 8.
Dong Qingli, Li Baoguo, Cai Jiayan, et al. Establishment of inactivation model for active *lactobacillus* numbers of bever-ages under cold temperature[J]. China Dairy Industry, 2009,37(5): 6 - 8. (in Chinese)

16 Braga R A, Fabbro I D, Borem F M, et al. Assessment of seed viability by laser speckle techniques [J]. Biosystems Engineering, 2003, 86(3):287 - 294.

17 胡孟晗,董庆利,刘宝林,等.基于计算机视觉的香蕉贮藏过程中颜色和纹理监测[J]. 农业机械学报,2013,44(8):180 - 184.
Hu Menghan, Dong Qingli, Liu Baolin, et al. Color and texture monitoring based on computer vision during banana storage[J]. Transactions of the Chinese Society for Agricultural Machinery, 2013,44(8): 180 - 184. (in Chinese)

18 Arizaga R, Trivi M, Rabal H. Speckle time evolution characterization by the co-occurrence matrix analysis[J]. Optics and Laser Technology, 1999,31(2): 163 - 169.

19 于智洋,刘志健.影响散斑激光散斑表面粗糙度测量的因素[J]. 黑龙江科技学院学报,2010,20(6): 460 - 462.
Yu Zhiyang, Liu Zhijian. Factors influencing laser speckle in surface roughness measurement [J]. Journal of Heilongjiang University of Science and Technology, 2010,20(6): 460 - 462. (in Chinese)

20 高雪,许尚忠,张英汉,等.影响牛肉品质的宰后因素[J]. 黄牛杂志,2004,30(1):26 - 29.
Gao Xue, Xu Shangzhong, Zhang Yinghan, et al. Factors affecting beef quality after slaughter[J]. Journal of Yellow Cattle Science, 2004,30(1): 26 - 29. (in Chinese)

21 Zdunek A, Adamiak A, Pieczywek P. The speckle method for the investigation of agricultural crops: a review[J]. Optics and Lasers in Engineering, 2014,52: 276 - 285.

(下转第 301 页)

173.
Huang Jianxi, Zhang Jie, Liu Junming, et al. Corrlation analysis between drought and winter wheat yields based on remotely sensed drought severity index[J]. Transactions of the Chinese Society for Agricultural Machinery, 2015, 46(3): 166 – 173. (in Chinese)
10 李克南,杨晓光,刘园,等. 华北地区冬小麦产量潜力分布特征及其影响因素[J]. 作物学报,2012,38(8):1483 – 1493.
Li Kenan, Yang Xiaoguang, Liu Yuan, et al. Distribution characteristics of winter wheat yield and its influenced factors in North China[J]. Acta Agronomice Sinica, 2012, 38(8): 1483 – 1493. (in Chinese)
11 姜亚珍, 张瑜洁, 孙琛,等. 基于 MODIS – EVI 黄淮海平原冬小麦种植面积分带提取[J]. 资源科学, 2015(2):417 – 424.
Jiang Yazhen, Zhang Yujie, Sun Chen, et al. MODIS – EVI based winter wheat planting information extraction of zoning on Huanghuaihai Plain[J]. Resources Science, 2015(2): 417 – 424. (in Chinese)
12 肖登攀, 陶福禄, 沈彦俊,等. 华北平原冬小麦对过去 30 年气候变化响应的敏感性研究[J]. 中国生态农业学报, 2014, 22(4):430 – 438.
13 冯玉梅. 鹤壁市旱灾成因及分析[J]. 科技风, 2008(9):5.
14 杨辉, 韩太国, 戴林森,等. 洛阳市小麦白粉病测报技术研究[J]. 洛阳农业高等专科学校学报, 2000, 2(2):17 – 18.
15 张金良, 张国海, 李留相,等. 洛阳地区干热风对小麦危害的分析及防御[J]. 河南科技大学学报:农学版, 1997, 3(4): 29 – 31.
16 于慧斌. 2009 年 10 月至 2010 年 4 月濮阳地区冬小麦冻(冷)害的发生与补救措施[J]. 农技服务, 2010, 27(11):1496 – 1497.
Yu Huibin. Winter wheat of frozen (cold) damage and remedial measures in Puyang from October 2009 to April 2010[J]. Serves of Agricultural Technology, 2010, 27(11): 1496 – 1497. (in Chinese)
17 林小惠, 王军邦, 李贵才,等. 基于 MODIS 遥感监测的东南亚地区植被动态[J]. 生态学杂志, 2011, 30(4):629 – 635.
Lin Xiaohui, Wang Junbang, Li Guicai, et al. Vegetation spatiotemporal variation in southeast Asia based on MODIS remote sensing monitoring[J]. Chinese Journal of Ecology, 2011, 30(4): 629 – 635. (in Chinese)
18 张明捷, 王运行, 赵桂芳,等. 濮阳冬小麦生育期气候变化及其对小麦产量的影响[J]. 中国农业气象, 2009, 30(2):223 – 229.
Zhang Mingjie, Wang Yunxing, Zhao Guifang, et al. Climate change during winter wheat growing period and its impacts on winter wheat yield in Puyang of Henan Province[J]. Chinese Journal of Agrometeorology, 2009, 30(2): 223 – 229. (in Chinese)
19 Zhang Yun, Gao J, Liu L, et al. NDVI-based vegetation changes and their responses to climate change from 1982 to 2011: a case study in the Koshi River Basin in the middle Himalayas[J]. Global and Planetary Change, 2013, 108(3): 139 – 148.
20 Liu Chun, Dong X, Liu Y, et al. Changes of NPP and their relationship to climate factors based on the transformation of different scales in Gansu, China[J]. CATENA, 2015: 190 – 199.
21 张戈丽,徐光良,周才平,等. 近 30 年来呼伦贝尔地区草地植被变化对气候的影响[J]. 地理学报,2011,66(1):47 – 58.

(上接第 294 页)

22 Briers J. Wavelength dependence of intensity fluctuations in laser speckle patterns from biological specimens[J]. Optics Communications, 1975, 13(3): 324 – 326.
23 Ye K, Wang H H, Zhang X X, et al. Development and validation of a molecular predictive model to describe the growth of *Listeria monocytogenes* in vacuum-packaged chilled pork[J]. Food Control, 2013, 32(1): 246 – 254.
24 Oulamara A, Tribillon G, Duvernoy J. Biological activity measurements on botanical specimen surfaces using a temporal decorrelation effect of laser speckle[J]. Journal of Modern Optics, 1989, 36(2): 165 – 179.
25 段怡婷. 生物散斑测量技术的研究[D]. 北京:北京交通大学, 2012.
Duan Yiting. Research of laser biospeckle measurement technology[D]. Beijing: Beijing Jiaotong University, 2012. (in Chinese)
26 Braga R A Jr, Borem F M, Rabelo G F, et al. Seeds analysis using bio-speckle[J]. Biosystems Engineering, 2003, 86(3): 287 – 296.
27 Botega J V L, Braga R A, Machado M P P, et al. Biospeckle laser portable equipment monitoring water behavior at coffee tree leaves[C]// Proc. SPIE 7387, Speckle 2010: Optical Metrology, 2010: 1 – 5.
28 石本义,毕坤,陈四海,等. 激光散斑技术在农产品检测中的应用[J]. 中国农学通报,2011,27(2):410 – 415.
Shi Benyi, Bi Kun, Chen Sihai, et al. Application of laser speckle technology on the detection of agricultural products[J]. Chinese Agricultural Science Bulletin, 2011, 27(2): 410 – 415. (in Chinese)
29 Cardoso R R, Costa A G, Nobre C M B, et al. Frequency signature of water activity by biospeckle laser[J]. Optics Communications, 2011, 284(8): 2131 – 2136.
30 Rabelo G F, Enes A M, Braga R A, et al. Frequency response of biospeckle laser images of bean seeds contaminated by fungi [J]. Biosystems Engineering, 2011, 110(3): 297 – 301.
31 孙志昶,冯晓琴,韩玲,等. 牦牛肉宰后成熟嫩化与细胞凋亡酶活力变化研究[J]. 农业机械学报,2014,45(1):191 – 197.
Sun Zhichang, Feng Xiaoqin, Han Ling, et al. Tenderness and apoptotic activity of yak meat during postmortem aging[J]. Transactions of the Chinese Society for Agricultural Machinery, 2014, 45(1): 191 – 197. (in Chinese)
32 Hughes J, Oiseth S K, Purslow P P, et al. A structural approach to understanding the interactions between colour, water-holding capacity and tenderness[J]. Meat Science, 2014, 98(3): 520 – 532.